IGARSS 2024 - 2024 IEEE International Geoscience and Remote Sensing Symposium | 979-8-3503-6032-5/24/$31.00 ©2024 IEEE | DOI: 10.1109/IGARSS53475.2024.10641037

NOVEL GNSS-R METHODS FOR FREEZE/THAW SURFACE STATE RETRIEVAL

H. Carreno-Luengo[1], C.S. Ruf[1], S. Gleason[2], A. Russel[1], A. Roy[3], and H. Salmabadi[3]

[1]Climate and Space Sciences and Engineering Department, University of Michigan (UMich)
[2]Daaxa LLC
[3]Université du Québec à Trois-Rivières

Ann Arbor, MI, United States of America (USA)
Email: {carreno,cruf}@umich.edu

ABSTRACT

Spatial and temporal patterns of landscape Freeze/Thaw (F/T) state transitions within the cryosphere are highly variable with impacts to climate, hydrological, ecological, and biogeochemical processes. F/T state has a strong impact on the seasonal amplitude and partitioning of surface energy exchange, while ecosystem responses to seasonal thaw are rapid, with evapotranspiration, soil respiration, and plant photosynthetic activity accelerating with warmer temperatures and the availability of liquid water. The annual thaw period also influences the vegetation growing season, while variability in F/T timing rules vegetation net primary production and Net Ecosystem CO2 Exchange (NEE) with the atmosphere. More than one third of the Earth's land surface is covered by seasonal or permanent soil frost. Many agricultural, engineering, and environmental issues and applications are affected by F/T state. A frozen land surface tends to reduce or even to impede water infiltration, which may promote flooding, surface runoff, and soil erosion.

In this work, Spire data through the NASA Commercial Smallsat Data Acquisition (CSDA) Program are used to develop novel Global Navigation Satellite Systems Reflectometry (GNSS-R) methods to determine the F/T state over the Arctic-Boreal region. The generated theoretical and experimental capabilities will be applied to analyze the spatial patterns and temporal dynamics with an improved spatio-temporal sampling as compared to Synthetic Aperture Radar (SAR) missions.

Index Terms— Freeze/Thaw, GNSS-R, Arctic-Boreal, Spire

1. INTRODUCTION

Detecting and quantifying rapidly changing F/T processes [1-3] at large scales requires spaceborne remote sensing observations. Landscape F/T is highly heterogeneous in both spatial and temporal domains, being affected by land cover type, Soil Moisture Content (SMC), topography, and microclimate [4]. Current and proposed SAR missions generate high spatial resolution (~ 100 m) but low temporal resolution (~ 7-14 days) measurements, which prevents observing the often-rapid F/T transitions. On the other hand, microwave radiometry missions provide high temporal resolution (~ 3 days) but low spatial resolution (~ 25 km), which prevents observing the landscape scale processes that directly affect F/T state [5-7]. Currently, there is no way to simultaneously monitor F/T state globally at appropriate spatial and temporal scales.

Brightness temperature, backscatter, and forward-scatter vary due to changes in the permittivity when water changes from liquid to solid and vice-versa. The soil permittivity (both real and imaginary parts) changes when the temperature goes from below 0°C to above 0°C. This process leads to changes in the reflectivity, and this is the fundamental basis of surface F/T state change detection. The permittivity of a thawed soil is much higher than that of a frozen soil. SMC and snow depth should be considered when analyzing this process. Microwave radiometry and SAR missions-derived measurements at several frequencies have been used to detect melt onset [8,9] and landscape F/T state [10,11]. However, there is ambiguity in the frequency dependent response of the microwave signal to various vertical components of the soil/snow/vegetation column. F/T transitions are directly related to the duration of snow cover [4,12]. However, separating the soil response is complicated, particularly in regions of forest vegetation [13-15].

The relatively recent era of spaceborne microwave measurements at L-band has shown a promising identification of soil F/T because of the strong sensitivity to soil permittivity, which is predominantly influenced by the phase of water, coupled with greater penetration depth through the vegetation and into the near soil surface than at higher frequencies (starting at C-band) from sensors such as e.g. the Advanced Microwave Scanning Radiometer-Earth Observing System (AMSR-E) [16]. Measurements with ground-based L-band radiometers have shown strong sensitivity to the surface F/T state [17-19], with algorithms

Authorized licensed use limited to: University of Michigan Library. Downloaded on December 04,2024 at 03:17:06 UTC from IEEE Xplore. Restrictions apply.

successfully scaled to satellite measurements from the Soil Moisture and Ocean Salinity (SMOS) mission [13,20]. High resolution L-band radar measurements from Phased Array type L-band Synthetic Aperture Radar (PALSAR) have been utilized to effectively show local scale variability in F/T transitions [21,22]. Data from the NASA (Satélite de Aplicaciones Científicas–D) SAC/D-Aquarius mission provided the initial opportunity to determine the continental scale L-band radar response to landscape F/T [23], but these measurements were constrained by very coarse spatial (~ 100 km) and temporal (weekly) resolutions. After the failure of the Soil Moisture Active Passive (SMAP) radar, one of the mission priorities was to develop the alternative F/T product using L-band radiometer brightness temperature [6].

2. FREEZE/THAW GNSS-R

GNSS-R is a sort of L-band passive multi-bistatic radar, with as many transmitters as navigation spacecrafts are in view. It provides global coverage, full temporal availability, and sampling of the Earth's surface over multiple tracks simultaneously within a wide area up to ~ 1,500 km. Several spaceborne experiments and missions have been deployed. Earth-reflected GNSS signals have sensitivity to a wide variety of geophysical parameters, such as, e.g., Snow Water Equivalent (SWE), SMC, vegetation parameters, and inland water bodies. More recently, some pioneering studies have shown a promising sensitivity to F/T transitions including SMAP GNSS-R mode [24,25], TechDemoSat-1 [26,27], and CYGNSS [28,29].

3. SPIRE GNSS-R DATA

Spire near-Nadir L1 dataset [30] is selected in this work for the study over the Arctic-Boreal region. Spire near-Nadir constellation is composed of 4 operational LEO CubeSats distributed in batch-1 (2 CubeSats, ~ 35° inclination, ~ 560 km altitude, peak science antenna gain ~9.5 dBi) and batch-2 (2 CubeSats, ~ 97° inclination, ~ 520 km altitude, peak science antenna gain ~8.5 dBi). Spire GNSS-R data are available through the NASA CSDA program. This multi-constellation dataset is generated with L-band GPS L1 C/A, Galileo E1 CA, Beidou B1 C_pilot, and QZSS L1 CA signals collected at Left Hand Circular Polarization (LHCP).

Data (May 2021-Present) are delivered with coherent integration time of 1 ms & incoherent integration time of 500 ms. Reflected signals are dynamically calibrated using direct GPS signals power measurements by an on-board receiver. The unique sampling properties of Spire will enable to further understand F/T dynamics, as well as the specification of requirements for future GNSS-R missions so as to fully exploit the multi-static capabilities of GNSS-R in such a way to generate the retrievals in a regular and more time-synchronized manner. As such, the outcome of this work is aimed to be highly relevant in both the GNSS-R and the wider remote sensing community.

4. MOTIVATION AND GOALS

The overarching goal of this project is on the use of Spire data to generate and optimize the theoretical and experimental capabilities required to monitor F/T state of the Arctic-Boreal region from high-inclination orbit GNSS-R missions. Observation of F/T state is highly relevant for quantifying carbon, energy, and water fluxes and how they affect land cover change.

This investigation is articulated through two specific goals:

Objective 1) Improve and validate state-of-the-art F/T retrieval algorithms using Spire data, including auxiliary data from microwave radiometry, so as to enhance the quality of the retrievals.

Objective 2) Analyze the spatial patterns and temporal dynamics at specific test sites and regional scales.

5. METHODOLOGY

The foundational retrieval scheme with Spire data is based on our existing F/T Seasonal Threshold Algorithm (STA). For a measurement at time t, the seasonal scale factor is defined as follows [28,29]:

$$\Delta(t) = \frac{\Gamma(\epsilon_s^*(t)) - \Gamma_{fr}}{\Gamma_{th} - \Gamma_{fr}} \quad (1)$$

where $\Gamma(\epsilon_s^*(t))$ is the reflectivity measurement estimated at time t, ϵ_s^* is soil permittivity, and Γ_{fr} and Γ_{th} are reflectivity measurements corresponding to frozen and thawed states.

6. PRELIMINARY RESULTS

Preliminary results are included in Fig. 1, after initial adjustment of our STA algorithm over the Arctic-Boreal region [28,29]. There are some similarities and some differences between the Spire, SMAP, ERA5-Land snow-based (frozen if snow cover > 10 %), and ERA5-Land air temperature-based (frozen if air temperature < -1° C) maps of annual frozen months. Overall, the Spire F/T map shows a good agreement with SMAP, including areas with dense vegetation such as boreal forests.

Currently, there are on-going cal/val activities over a variety of test sites for enhanced interpretation of the results, and potential further adjustment and optimization of the retrieval algorithm over heterogeneous scenes.

7. REFERENCES

[1] B.P. Selvam, H. Laudon, F. Guillemette, M. Berggren, "Influence of Soil Frost on the Character and Degradability of Dissolved Organic Carbon in Boreal Forest Soils," Journal Geophysical Research Biogeosciences, vol. 121, no. 3, pp. 829-840, 2016, https://doi.org/10.1002/2015JG003228

Authorized licensed use limited to: University of Michigan Library. Downloaded on December 04,2024 at 03:17:06 UTC from IEEE Xplore. Restrictions apply.

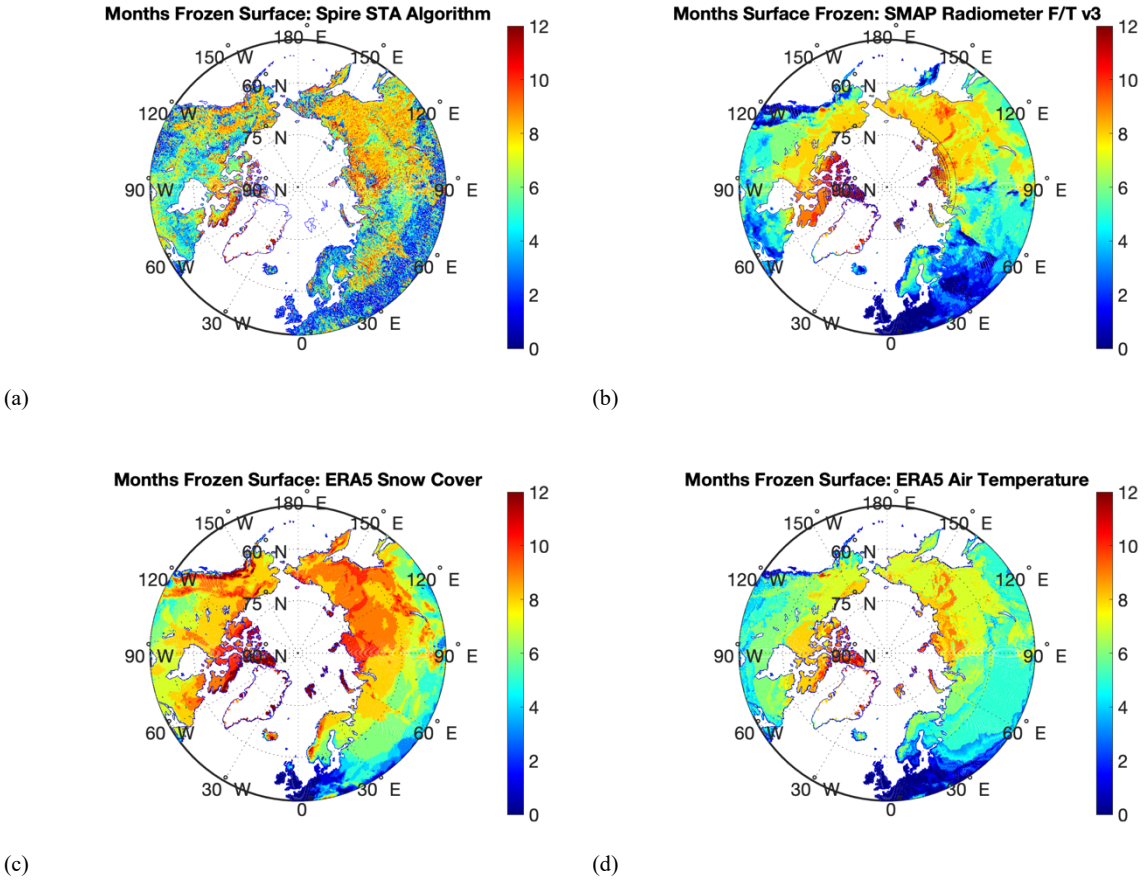


Fig. 1. Number of frozen months in 2022 derived by: (a) Initial results with Spire F/T Seasonal Threshold Algorithm (STA) [28,29]. (b) SMAP Enhanced L3 Radiometer Global and Northern Hemisphere Daily 9 km EASE-Grid Freeze/Thaw State, Version 3. (c) ERA5-Land snow cover (frozen if snow cover > 10 %). (d) ERA5-Land air temperature (frozen if air temperature < -1° C).

[2] M.L. Goulden, S. Wofsy, J. Harden, S. Trumbore, P. Crill, S. Gower, T. Fries, B. Daube, S. Fan, D. Sutton, A. Bazzaz, and J. Munger, "Sensitivity of Boreal Forest Carbon Balance to Soil Thaw," Science, vol. 279, no. 9, pp. 214-217, 1998, https://www.science.org/doi/10.1126/science.279.5348.214

[3] L. Oygarden, "Rill and Gully Development During an Extreme Winter Runoff Event in Norway," CATENA, vol. 50, no. 2-4, pp. 217-242, 2003, https://doi.org/10.1016/S0341-8162(02)00138-8

[4] J.S. Kimball, K.C. McDonald, S. Frolking, and S.W. Running, "Radar Remote Sensing of the Spring Thaw Transition Across a Boreal Landscape," Remote Sensing of Environment, vol. 89, no. 2, pp. 163-175, 2004, https://doi.org/10.1016/j.rse.2002.06.004

[5] Y. Kim, J.S. Kimball, K. Zhang, K.C. McDonald, "Satellite Detection of Increasing Northern Hemisphere Non-Frozen Seasons from 1979 to 2008: Implications for Regional Vegetation Growth," Remote Sensing of Environment, vol. 121, pp. 472-487, 2012, https://doi.org/10.1016/j.rse.2012.02.014

[6] C. Derksen, X. Xu, R.S. Dunbar, A. Colliander, Y. Kim, J.S. Kimball, T.A. Black, E. Euskirchen, A. Langlois, M.M. Loranty, P. Marsh, K. Rautiainen, A. Roy, and J. Stephen, "Retrieving Landscape Freeze/Thaw State from Soil Moisture Active Passive (SMAP) Radar and Radiometer Measurements," Remote Sensing of Environment, vol. 194, no. 1, pp. 48-62, 2017, https://doi.org/10.1016/j.rse.2017.03.007

[7] J. Obua, S. Westermanna, A. Bartschb, N. Berdnikovc, H.H. Christiansend, A. Dashtserene, R. Delaloyef, B. Elberlingg, B. Etzelmüllera, A. Kholodovh, A. Khomutovc, A. Kääba, M.O. Leibmanc, A.G. Lewkowiczi, S.K. Pandah, V. Romanovskyh, R.G. Wayk, A. Westergaard- Nielseng, T. Wum, J. Yamkhine, and D. Zoum, "Northern Hemisphere Permafrost Map Based on TTOP Modelling for 2000–2016 at 1 km^2 Scale," Earth-Sciences Reviews, vol. 193, pp. 299-316, 2019, https://doi.org/10.1016/j.earscirev.2019.04.023

[8] L. Wang, C. Derksen, and R. Brown, "Recent Changes in Pan-Arctic Melt Onset from Satellite Passive Microwave Measurements," Geophysical Research Letters, vol. 40, no. 3, pp. 522-528, 2013, https://doi.org/10.1002/grl.50098

[9] J. Mortin, T. Schrøder, A.W. Hansen, B. Holt, and K.C. McDonald, "Mapping of Seasonal Freeze-Thaw Transitions Across the Pan-Arctic Land and Sea Ice Domains with Satellite Radar," Journal Geophysical Research, vol. 117, C8, 2012, https://doi.org/10.1029/2012JC008001

Authorized licensed use limited to: University of Michigan Library. Downloaded on December 04,2024 at 03:17:06 UTC from IEEE Xplore. Restrictions apply.

[10] A. Bartsch, R. Kidd, W. Wagner, and Z. Bartalis, "Temporal and Spatial Variability of the Beginning and End of Daily Spring Freeze/Thaw Cycles Derived from Scatterometer Data," Remote Sensing of Environment, vol. 106, no. 3, pp. 360-374, 2007, https://doi.org/10.1016/j.rse.2006.09.004

[11] S.M. Bateni, C. Huang, S. Margulis, E. Podest, and K.C. McDonald, "Feasibility of Characterizing Snowpack and the Freeze-Thaw State of Underlying Soil Using Multifrequency Active/Passive Microwave Data," IEEE Transactions on Geoscience and Remote Sensing, vol. 51, no. 7, pp. 4085-4102, 2013, https://ieeexplore.ieee.org/document/6423890

[12] J. Kimball, K.C. McDonald, A Keyser, S. Frolking, and S. Running, "Application of the NASA Scatterometer (NSCAT) for Classifying the Daily Frozen and Non-Frozen Landscape of Alaska," Remote Sensing of Environment, vol. 75, no. 1, pp. 113-126, 2001, https://doi.org/10.1016/S0034-4257(00)00160-7

[13] A. Colliander, K.C. McDonald, R. Zimmermann, R. Schroeder, J. Kimball, and G. Njoku, "Application of QuikSCAT Backscatter to SMAP Validation Planning: Freeze/Thaw State over ALECTRA Sites in Alaska from 2000 to 2007," IEEE Transactions on Geosciences and Remote Sensing, vol. 50, no. 2, pp. 461-468, 2012, https://ieeexplore.ieee.org/abstract/document/6112797

[14] A. Roy, A. Royer, C. Derksen, L. Brucker, A. Langlois, A. Mialon, and Y. Kerr, "Evaluation of Spaceborne L-band Radiometer Measurements for Terrestrial Freeze/Thaw Retrievals in Canada," IEEE Journal of Selected Topics in Applied Earth Observations and Remote Sensing, vol. 8, no. 9, pp. 4442-4459, 2015, https://ieeexplore.ieee.org/abstract/document/7274330

[15] L. Farhadi, R. Reichle, G. DeLannoy, and J. Kimball, "Assimilation of Freeze–Thaw Observations into the NASA Catchment Land Surface Model," Journal Hydrometeorology, vol. 16, no. 2, pp. 730-743, 2015, https://doi.org/10.1175/JHM-D-14-0065.1

[16] M. Watanabe, G. Kadosaki, Y. Kim, M. Ishikawa, K. Kushida, Y. Sawada, T. Tadono, M. Fukuda, and M. Sato, "Analysis of the Sources of Variation in L-band Backscatter from Terrains with Permafrost," IEEE Transactions on Geoscience and Remote Sensing, vol. 50, no. 1, pp. 44-54, 2011, https://ieeexplore.ieee.org/document/5959203

[17] M. Schwank, M. Stähli, H. Wydler, J. Leuenberger, C. Mätzler, and H. Flühler, "Microwave L-band Emission of Freezing Soil," IEEE Transactions on Geoscience and Remote Sensing, vol. 42, no. 6, pp. 1252-1261, 2004, https://ieeexplore.ieee.org/document/1304892

[18] K. Rautiainen, J. Lemmetyinen, J. Pulliainen, J. Vehviläinen, M. Drusch, A. Kontu, J. Kainulainen, and J. Seppänen, "L-Band Radiometer Observations of Soil Processes in Boreal and Subarctic Environments," IEEE Transactions on Geoscience and Remote Sensing, vol. 50, no. 5, pp. 1483-1497, 2012, https://ieeexplore.ieee.org/document/6046126

[19] K. Rautiainen, J. Lemmetyinen, M. Schwank, A. Kontu, C. Menard, C. Mätzler, M. Drusch, A. Wiesmann, J. Ikonen, and J. Pulliainen, "Detection of Soil Freezing from L-Band Passive Microwave Observations," Remote Sensing of Environment, vol. 147, pp. 206-218, 2014, https://doi.org/10.1016/j.rse.2014.03.007

[20] K. Rautiainen, T. Parkkinen, J. Lemmetyinen, M. Schwank, A. Wiesmann, J. Ikonen, C. Derksen, S. Davydov, A. Davydova, J. Boike, M. Langer, M. Drusch, and J. Pulliainen, "SMOS Prototype Algorithm for Detecting Autumn Soil Freezing," Remote Sensing of Environment, vol. 180, pp. 346-360, 2016, https://doi.org/10.1016/j.rse.2016.01.012

[21] E. Podest, K.C. McDonald, and J. Kimball, "Multisensor Microwave Sensitivity to Freeze/Thaw Dynamics Across a Complex Boreal Landscape," IEEE Transactions on Geoscience and Remote Sensing, vol. 52, no. 11, pp. 6818-6828, 2014, https://ieeexplore.ieee.org/document/6780599

[22] J. Du, J. Kimball, M. Azarderakhsh, R.S. Dunbar, M. Moghaddam, and K.C. McDonald, "Classification of Alaska Spring Thaw Characteristics Using Satellite L-band Radar Remote sensing," IEEE Transactions on Geoscience and Remote Sensing, vol. 53, no. 1, pp. 542-556, 2014, https://ieeexplore.ieee.org/document/6825807

[23] X. Xu, C. Derksen, S. Yueh, R.S. Dunbar, and A. Colliander, "Freeze/Thaw Detection and Validation Using Aquarius L-band Backscattering Data," IEEE Journal of Selected Topics in Applied Earth Observations and Remote Sensing, vol. 9, no. 4, pp. 1370-1381, 2016, https://ieeexplore.ieee.org/document/7409984

[24] H. Carreno-Luengo, S.T. Lowe, C. Zuffada, S. Esterhuizen, and S. Oveisgharan, "Spaceborne GNSS-R from the SMAP Mission: First Assessment of Polarimetric Scatterometry over Land and Cryosphere," MDPI Remote Sensing, vol. 9, pp. 362, 2017, https://doi.org/10.3390/rs9040362

[25] C. Chew, S.T. Lowe, N. Parazoo, S. Esterhuizen, S. Oveisgharan, E. Podest, C. Zuffada, and A. Freedman, "SMAP Radar Receiver Measures Land Surface Freeze/Thaw State Through Capture of Forward-Scattered L-Band Signals," Remote Sensing of Environment, vol. 198, pp. 333-344, 2017, https://doi.org/10.1016/j.rse.2017.06.020

[26] D. Comite, L. Cenci, A. Colliander, and N. Pierdicca, "Monitoring Freeze-Thaw State by Means of GNSS Reflectometry: An Analysis of Techdemosat-1 Data," IEEE Journal of Selected Topics in Applied Earth Observations and Remote Sensing, vol. 13, pp. 2996-3005, 2020, https://ieeexplore.ieee.org/document/9103273

[27] K. Rautiainen, D. Comite, J. Cohen, E. Cardellach, M. Unwin, and N. Pierdicca, "Freeze-Thaw Detection over High-Latitude Regions by Means of GNSS-R Data," IEEE Transactions on Geoscience and Remote Sensing, vol. 60, 2021, https://ieeexplore.ieee.org/document/9600803

[28] H. Carreno-Luengo, and C. Ruf, "Retrieving Freeze/Thaw Surface State from CYGNSS Measurements," IEEE Transactions on Geoscience and Remote Sensing, vol. 60, 2021, https://ieeexplore.ieee.org/document/9576723

[29] H. Carreno-Luengo, and C. Ruf, "Mapping Freezing and Thawing Surface State Periods with the CYGNSS Based F/T Seasonal Threshold Algorithm," IEEE Journal of Selected Topics in Applied Earth Observations and Remote Sensing, vol. 15, pp. 9943-9952, 2022, https://ieeexplore.ieee.org/document/9926088

[30] P. Jales, V. Irisov, J. Mashburn, J. Cartwright, T. Yuasa, and V. Freeman, "Spire Near-Nadir GNSS-R Level 1 Version 1.3 Product Manual," Spire Global Inc., 2023.

Acknowledgements

This research was supported in part by the NASA Science Mission Directorate contract 80LARC21DA003 with the University of Michigan.

Authorized licensed use limited to: University of Michigan Library. Downloaded on December 04,2024 at 03:17:06 UTC from IEEE Xplore. Restrictions apply.